MICROSCOPIC STUDY OF CRACKING AND WEAR MECHANISMS IN 2D RANDOMLY CHOPPED AND 3D NON-WOVEN C/C COMPOSITES

Soydan Ozcan and Peter Filip*
Center for Advanced Friction Studies
Southern Illinois University at Carbondale
Carbondale, IL, 62901-4403, USA

Corresponding author e-mail address:filip@siu.edu

Introduction

Carbon-carbon composite friction materials (C/C) represent one of the most important elements of aerospace, military and higher-end commercial vehicle brakes. Since 1960s, they underwent significant development and improvement. The wear and friction mechanisms, however, remain unclear and require additional attention in order to improve the braking effectiveness and transportation safety. This paper deals with two commercially available C/C materials and, by addressing the impact of microstructure parameters on fracture and wear, it contributes to understanding of wear phenomena in C/C ceramics.

Experimental

The analyzed C/C composite materials were provided by Honeywell International. Two types of C/C composites were used in this study. Two dimensional (2D) randomly chopped pitch fiber in charred resin matrix and three dimensional (3D) non-woven pan fiber in CVI matrix. A Nikon light microscope (polarized light, Microphot-FX) SEM (Hitachi S 570) and TEM (Hitachi H 7100) equipped with EDX analyzer were used for microstructure characterization. The four-point bending tests were performed according to the ASTM standards (E-855-90) using the Instron Mechanical Testing System 4206. Nanoindentation measurements were made using a Nanoindenter XP system (MTS Nanoinstruments, Knoxville, TN) with Berkovich type diamond indenter. Standardized procedures were used for sample preparation [1 - 5].

Results and Discussion

Wear characteristics of 2D (HWCCA) and 3D (HWCCD) materials are shown in Fig. 1. More extensive wearing of 3D sample is particularly obvious at lower friction energies, simulating 12.5, 25 and 50% of normal loading energy (NLE), respectively. It is easily seen that almost 100% difference in wear was detected at lower energies dissipated in the friction process.

Microstructures of the two investigated materials are significantly different as obvious from light microscopy images shown in Fig. 2. The 2D sample consists of randomly

chopped pitch fiber boundless embedded in a charred resin matrix and finally densified by two CVI processes leading to the formation of different degree of anisotropy.

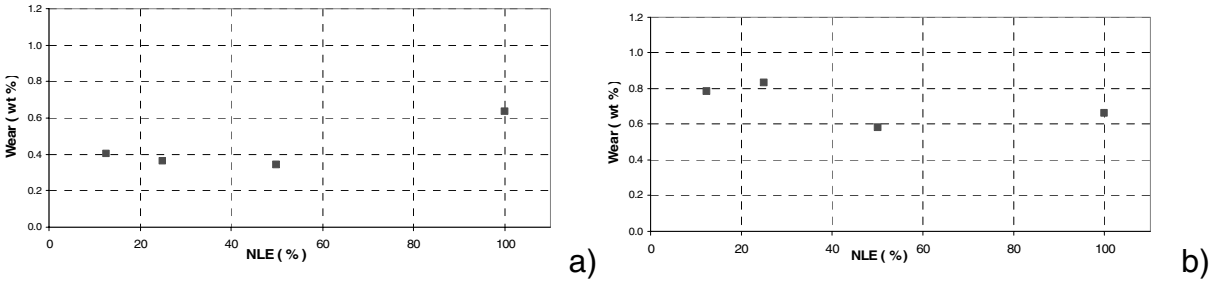

Figure 1. Wear of two investigated samples 2D (a) and 3D (b).

The 3D material is typified by the presence of pan fiber, partly oriented in z direction (perpendicular to the friction surface, not shown). The activity of the optical regions is correlated with the orientation of the crystallinity of graphite lamellae. In this study, distinctions of the anisotropic CVI carbon was explained by measuring the extinction angles of each CVI and the optical textures are inferred according to the classification of Bourrat [1] and Duppel [1, 2].

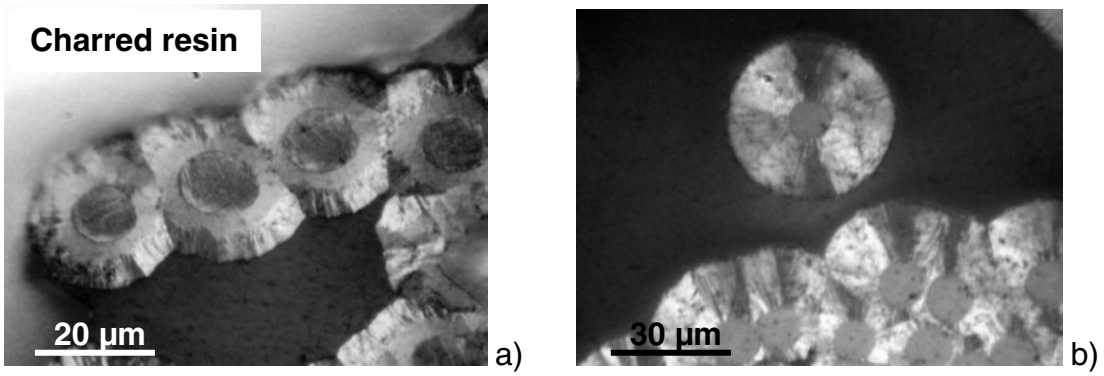

Figure 2. Microstructure of 2D (a) and 3D (b) material as seen in polarized light microscope.

Figures 3 a and b show the high magnification TEM bright field images and selected area diffraction patterns (SAED) corresponding to fiber, matrix and interface areas. Determination of the texture degree obtained by the measurement of the orientation angle (OA) in (002) diffraction pattern [3, 4]. The pitch fiber in 2D composite consist of highly textured (rough laminar) microstructure with OA = 30° (Fig. 3a), while the pan fiber in 3D sample exhibited slightly less ordered microstructure with OA = 45° (Fig 3b). On contrary the matrix of 2D material was less organized (OA = 80°) compared to 3D sample matrix (OA = 85°). The fiber/matrix interface is stronger in 3D material, which forms semi-crystalline interphase (Fig. 3b).

Different Mechanical Properties of investigated materials were detected in nanoindentation (Fig. 4) and four point bending (Fig. 5) experiments.

Figure 4a summarizes the “nanohardness results” from 10 measurements performed with 2D and 3D samples.

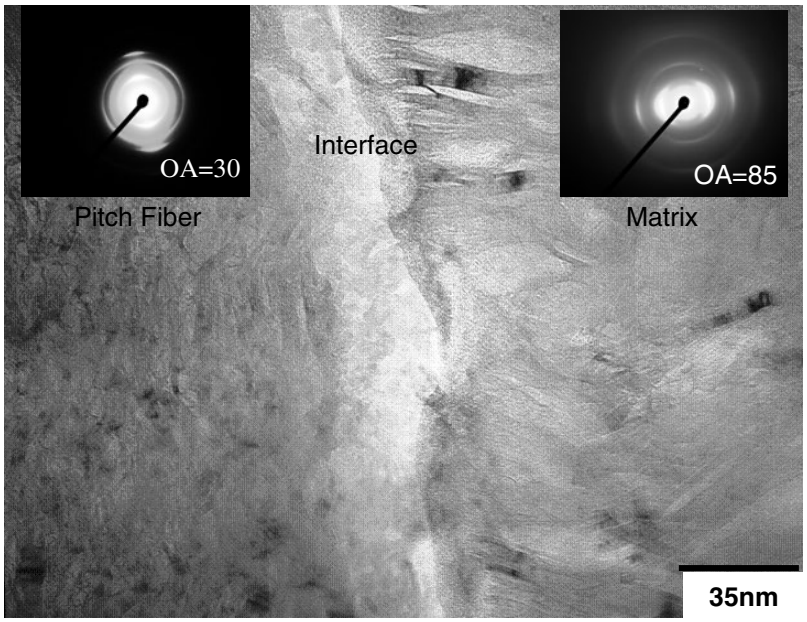

Figure 3a. TEM bright field image of 2D material. The inserts represent SAED patterns from the fiber (left part of the image) and matrix (right part) areas, respectively.

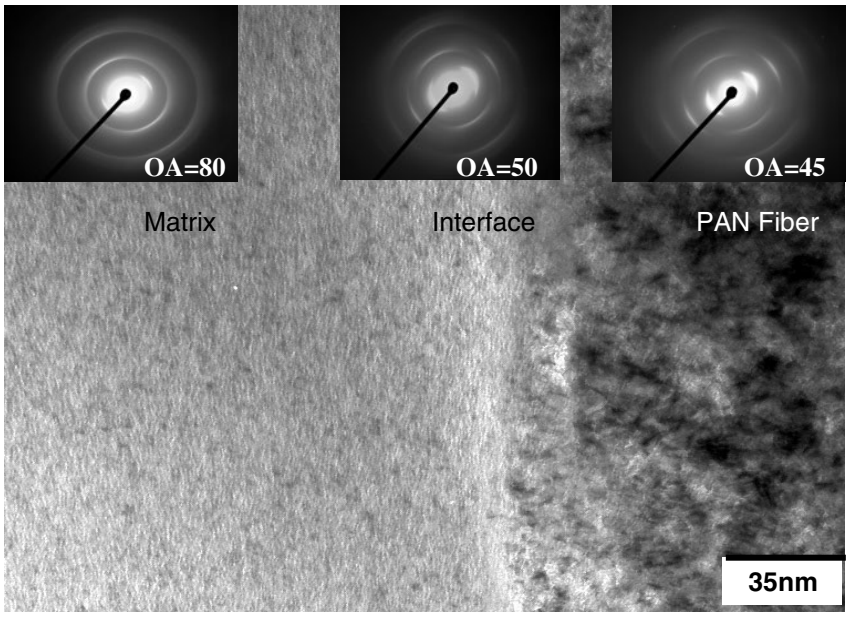

Figure 3b. TEM bright field image of 3D material. The inserts represent SAED patterns from the fiber (left part of the image) and matrix (right part) areas, respectively. A semi-crystalline interphase formed between C-fiber and CVI matrix.

As apparent from Fig 4b, fracturing occurred during indentation and these data can be used for comparison between 2D and 3D materials only. “Nanohardness” of 2D material is higher compared to 3D sample.

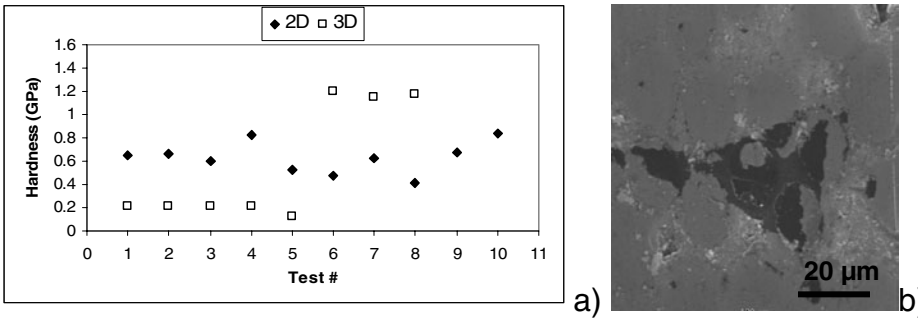

Figure 4. Nanoindentation results (a) and characteristic indent shape (b).

The load-displacement curves obtained from the four-point bending tests are plotted in Figs. 5a (2D sample) and 5b (3D material). It can be easily seen, that the load-displacement curve is almost linear up to the when maximum force occur. For 2D composite, fracturing was observed at lower displacement (0.2 – 0.4 mm), in contrast with 3D (0.8 – 1.0 mm). The amount of energy dissipated during fracturing (corresponds to the area beneath Load – Displacement curve) is higher in 3D sample compared to 2D material. On the other hand, the strength of 2D samples (maximum load before fracture) is higher than strength of 3D material.

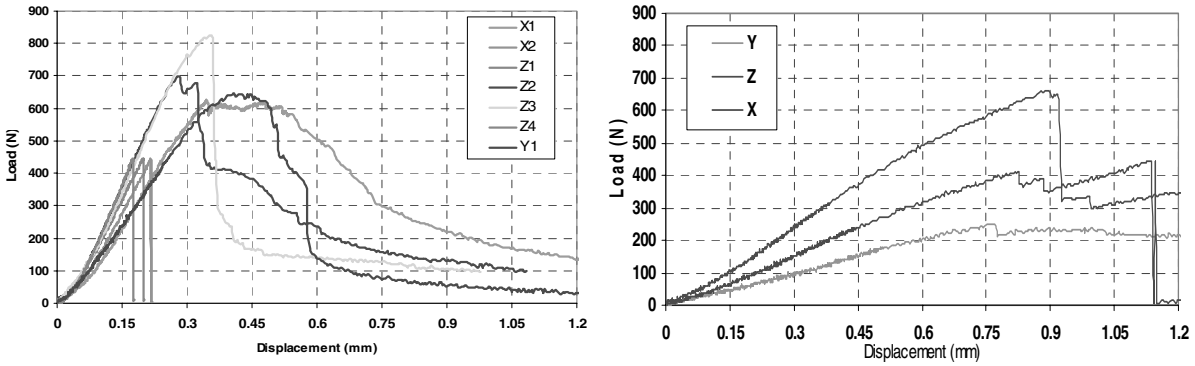

Figure 5. Load – displacement dependences as detected in four point bending tests for 2D (a) and 3D (b) material.

Micromechanisms of failure during four point bending were revealed SEM analysis (Fig. 6). The fracturing mechanism in 2D materials is typified by deflection of microcracks on fiber/matrix interface. This interface is weak as obvious from TEM analysis (Fig. 3a). Correspondingly, an extensive pull-of phenomenon was detected on the fractured surfaces (Fig. 6a). In contrast, the 3D material with stronger fiber/matrix interaction exhibited fracturing mechanisms typified by shearing and cracking between CVI layers with different textures and crack deflection along individual CVI layers (Figs. 6 b and c). Crack bridging within textured CVI levels is always detected on 3D sample fractured surfaces. The intensity of these effects increases with increasing load (energy) spent in

damaging process. Crack deflection on fiber/matrix interface was seen only rarely in 3D samples due to a very good cohesion and formation of interphase between fiber and matrix (Fig. 3b).

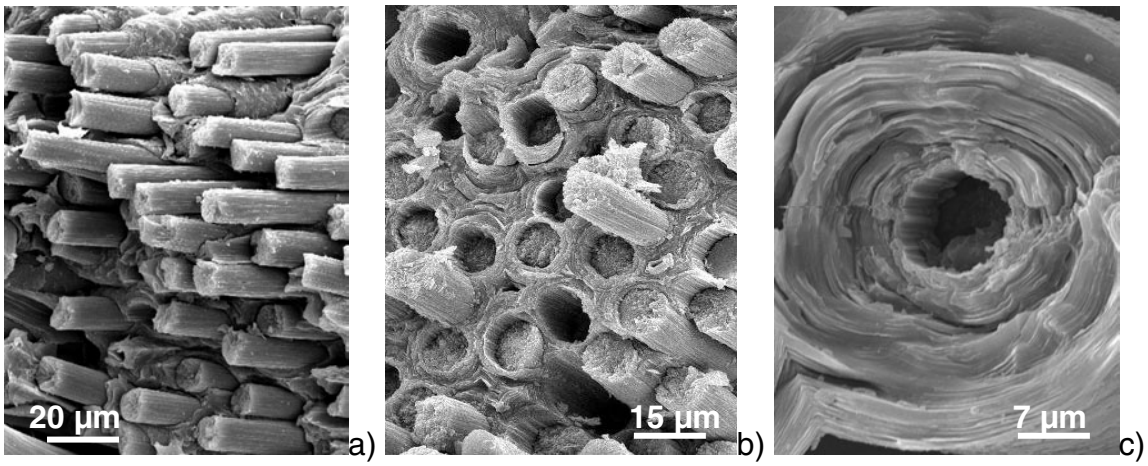

a) b) c)

Figure 6. The fracture surface of 2D sample (a) and 3D sample (b) and detail in (c).

Apparently, the different detected mechanisms yield an easier fracturing of 3D material on the micro structural level. The overall moduli of elasticity of both 2D and 3D materials are similar (10 to 12 GPa) and apparently do not have significant impact on micro mechanisms of crack formation and wear.

When the 2D and 3D materials are compared, it is obvious that 3D sample is typified by i) less organized structure of C fiber (Fig. 3b); ii) better organized microstructure of matrix (Fig. 3b) (structural organization is considered to be worst for amorphous glassy carbon and best for graphitic structure without defects), iii) stronger fiber/matrix interaction (cohesion or strength) (Fig. 3b); iv) lower hardness (Fig. 4) and different fracturing mechanisms (Figs. 5 and 6).

Apparently, the lower detected hardness of 3D material compared to 2D sample can be related to discussed microstructure differences. In combination with an easier fracturing, the increased wear observed in 3D composite can be easily explained.

More extensive wearing of 3D sample is particularly obvious at lower friction energies, simulating 12.5, 25 and 50% of normal loading energy (NLE), respectively. A systematic TEM analysis of friction layer developed on the friction surface of investigated samples revealed that 3D samples always exhibit the presence of an amorphous friction layer (Fig. 7). In contrast with 3D sample, 2D materials are characteristic by development of semi-crystalline friction layers (Fig. 8).

As obvious from TEM images, the friction layer consists of more or less sintered fine wear particles. Micro and nano-fracturing mechanisms are apparently the dominant factor leading to the formation of fine particulates resembling the friction layer.

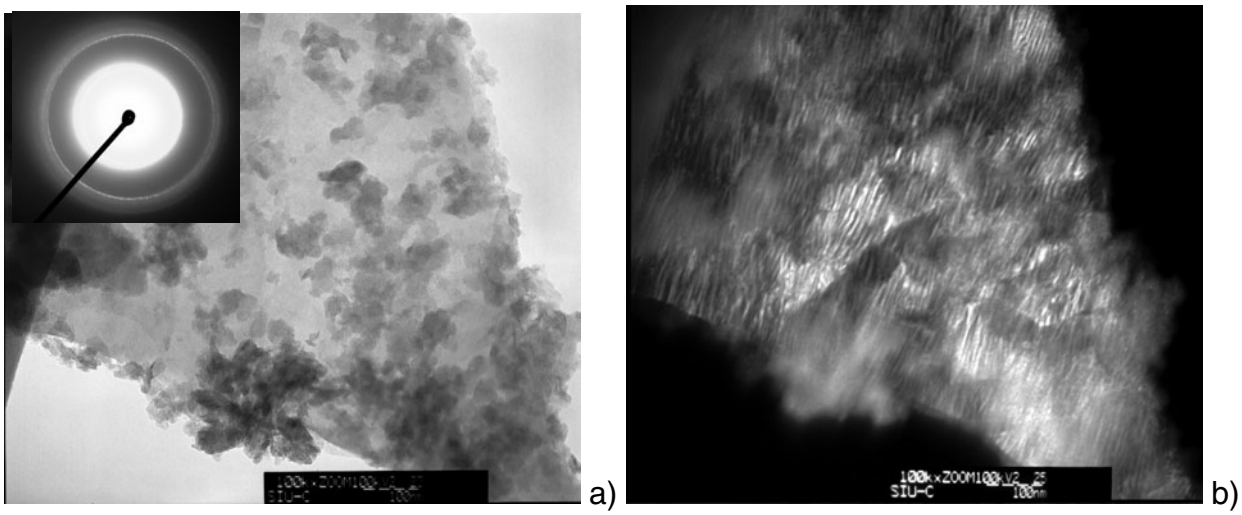

Figure 7. Bright field TEM image of semi-crystalline friction layer generated on the surface of 2D sample (a), diffraction pattern (insert in a) from the central part of (a), and dark field image (b).

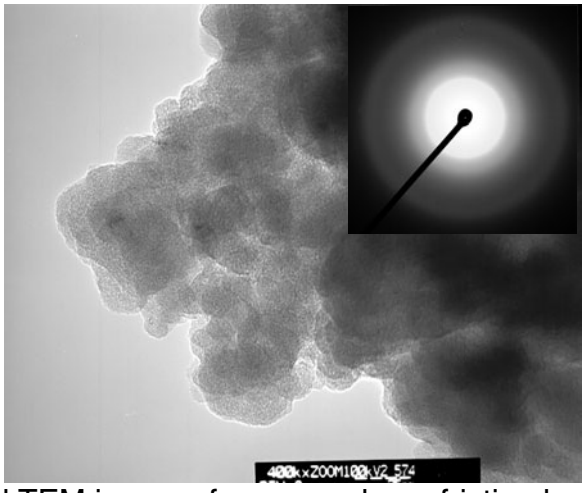

Figure 8. Bright field TEM image of an amorphous friction layer generated on the surface of 3D sample. Insert represents the diffraction pattern taken from the central part of the layer.

However, the more organized structure of C fiber and 2D architecture may have an impact on crystallinity of the layer. Further studies are required in order to provide a detailed explanation of observed interface phenomena. At 100% NLE conditions, both 3D and 2D samples exhibited fully amorphous structure. Correspondingly, the wear is similar in both materials at 100% NLE. Apparently, the intensity of cracking and defect introduction increases with increasing energy dissipated during the friction process. Since the surface roughness data indicated only minor differences between investigated 3D and 2D samples, it is assumed that the character of the friction layer is responsible for differences in wear rate.

The impact of microstructure of the bulk on wear characteristics is obvious. The differences of thermal properties (not shown here) also play a significant role.

Temperatures achieved on the surface of 2D materials are considerably higher and may contribute to the particular character of fracturing and friction layer formation.

Conclusions

1.) Microstructure of C/C composites and their microstructure has significant effect on wear of C/C materials. The impact is more obvious at lower energies applied in the presented testing program. Approximately 100% difference in wear was detected when 3D (higher wear) and 2D (lower wear) samples were compared.
2.) Friction layer developed on the friction surface seems to be the major factor responsible for different wear of samples. This layer consists of crushed and/or sintered fine particulates. Apparently the cracking/fracturing mechanisms have an impact on the friction layer formation.
3.) 2D samples with semi-crystalline friction layer (better organized carbon) exhibited significantly lower wear compared to 3D materials which were always covered by an amorphous friction layer.
4.) Moduli of elasticity do not have significant impact on micro mechanisms of crack formation (and wear).
5.) It is obvious that by understanding the mechanisms of wear and friction layer formation, it is possible to optimize the bulk microstructure of C/C composites.

References

[1] Bourrat X., Trouvat B., Limousin G. and Vignoles G., Pyrocarbon anisotropy as measured by electron diffraction and polarized light. Journal of Materials Research. 2000:15(1): 92-101.
[2] Duppel P, Bourrat X, Pailler R. Structure of pyrocarbon infiltrated by pulse-CVI. Carbon 1995:33(9):1193-204.
[3] Tressaud V, Chambon M, Gupta V, Flandrois S, and Bahl O. P, Fluorine-intercalated carbon fibers III. A transmission electron microscopy study. Carbon 1995:33(9): 1339-1345.
[4] Reznik B.Huttinger KJ. On the terminology for pyrolitic carbon. Carbon 2002:40(4): 621-624.
[5] Hoffman G., Wiedenmeier M., Freund M., Beavan A., Hay J., Pharr G. M., An investigation of the relationship between position wothin coater and pyrolitic carbon characteriastics using nanoindentation, Carbon 2000: 38 (5): 645-653.

Acknowledgement

This research was sponsored by NSF (Grant EEC 9523372), State of Illinois and consortium of twelve industrial partners (www.frictioncenter.com).